RECENT ADVANCES IN MATERIALS MANUFACTURING AND MACHINE LEARNING PROCESSES

Edited by
Dr Bjorn Schuller, Dr. Rajiv Gupta, Dr. Rakesh Mote,
Dr. Abhishek Sharma, Dr. J.P.Giri, Dr. R.B. Chadge

CRC CRC Press
Taylor & Francis Group

Contents

Chapter 3

Metal inert gas cladding simulations and residual stress analysis of mild steel

Arka Banerjee[a], Rajeev Ranjan[b], Manoj Kundu[c] and Subhas Chandra Moi[d]

Department of Mechanical Engineering, Dr. B. C. Roy Engineering College, Durgapur, West Bengal, India

Abstract

In this article, residual stress analysis and mathematical modeling for mild steel cladding applied by metal inert gas welding are presented. To determine the features of residual stresses, several cladding materials and varying process parameters are applied on mild steel. Simulating the cladding process involves using element birth and death function of ANSYS software. Firstly, ANSYS top-down technique is used to build geometry. To make brick meshing of the geometry easier, the geometry is separated. Thermal analysis is initially performed using the proper elements to determine the temperature distribution during the cladding process. In order to determine the nature of the residual stress, coupled field analysis is performed after the structure has been cooled to its original temperature (no load condition). The authors noted that several clad materials were proposed by earlier research to reduce the coating's residual stress. This study primarily emphasises the impact of clad thickness on residual stress for the substrate of mild steel and recommends the appropriate settings for the least amount of residual stress. The findings show that the residual stress decreases with decreasing clad material thickness.

Keywords: ANSYS, finite element analysis, MIG cladding, residual stresses

Introduction

Obtaining a material with the desired qualities is challenging. Hardness, yield strength, corrosion, and wear resistance of a material play significant roles in structural design and the lifespan of a product. Corrosion in machine components leads to considerable reduction in their service life [1, 2]. Corrosion is chemical hazard to a material due to unavoidable environmental conditions, which is very common in industries like nuclear power plant, petrochemical industries, fertiliser industries, food processing and chemical, industries etc [3-6]. However, materials with the qualities are pricey. As a result, their price will increase if they are used to make components. The procedure of surface treatment is utilised to get around this sort of issue so that the service life of a component may be improved while keeping the cost of the material acceptable. Consequently, cladding is carried out to enhance the necessary properties on the surface of the base metal. In cladding, an inexpensive substrate is covered with a layer of a hard or corrosion-resistant alloy to boost a component's hardness, corrosion resistance and wear resistance with the goal of extending the component's service life [7-8]. Welding is a potential candidate for the cladding process because of the availability wide range of processes to cater the needs of the different industries [9]. Diverse welding techniques, such as TIG, MIG, SMAW, SAW, FCAW, PTAW, and laser deposition can be used to apply cladding [10]. During the MIG welding procedure, which joins the two base materials, welding cannon feeds a continuous solid wire electrode into the weld pool. To prevent contamination of the weld pool, a shielding gas is further provided through the welding gun. The term MIG really stands for metal inert gas. Its vernacular name is wire welding, while its scientific name is gas metal arc welding (GMAW) [11-12]. Manual MIG welding is frequently referred to as a semi-automatic process since the arc length and wire feed are controlled by the power source, but the wire position and travel speed are manually controlled. When none of the process parameters are directly under the control of a welder, the process can also be automated; welding may still need manual adjustments. Welding can be considered as automated when no manual assistance is required. [13-14]. In order for the process to function, the wire must be positively charged and connected to a power source that offers a constant voltage. The choice of wire feed rate and wire diameter determine the welding current since the burn-off rate of the wire will stabilise with the feed rate [15-18]. Finite element studies are frequently used as the basis for numerical assessments of cladding residual stresses [19]. The authors note that earlier research on the metal inert gas cladding approach recommended different coating materials to reduce residual stress. However, the present article investigated the variation of residual stresses on the clad thickness.

Cladding residual stresses

Even in the absence of external loads or heat gradients, residual stresses that persist, especially in welded components, cause considerable plastic deformation, which causes warping and distortion of an item.

[a]arka.banerjee@bcrec.ac.in, [b]rajeevranjan.br@gmail.com, [c]manoj.kundu@bcrec.ac.in, [d]subhas.moi@bcrec.ac.in

Temperature affects the residual strains on the cladding, which decrease with rising temperatures. The amount and distribution of residual stresses in the cladding are influenced by the cladding's thickness, geometry, base metal and cladding material characteristics, heat and pressure treatments used before and after the cladding process, and geometry of the cladded component. These residual stresses are intricate and frequently assessed using computer modelling and tests [20-21]. The basis for experimental assessments frequently stems from tests carried out in the lab on specimens that were fabricated from cladded parts. To determine the through-thickness residual stresses, experimental methods that entail cutting and machining the plate must be destructive. They are based on relaxation technique. Surface strain gauges are used to keep track of the deformations that occur during each cutting and machining phase. These deformations serve as the input for a computational process that determines the residual stresses present in the cladded plate prior to cutting. The size and distribution of cladding residual stresses are affected by several temperature dependent characteristics, though; therefore, computer simulations are often carried out under certain over-simplified assumptions.

Numerical methods

Residual stress and temperature distribution in the clad and parent materials are to be determined. For this analysis, initially the temperature is at 200°C. Bottom side of the base material is considered to be insulated, at the top surface convection is considered. To find out the temperature distribution, a transient thermal analysis is required. As the initial condition for the geometry in the thermal analysis, a uniform temperature of 1800°C.is used. Step size is chosen as 0.5 sec for the optimisation of the calculation time. To get the residual stress, the geometry has been cooled down to the initial temperature.

FEM based analysis has been carried out using ANSYS thermal-structural coupled analysis [22]. The material is considered as homogeneous for the structural analysis. Other material properties for parent and clad material are given in Table 3.1.

Brick mesh has been used to discretise entire geometry; total numbers of cells are 4500. In the thermal-structural coupled analysis calculated thermal results are used by the solver for structural analysis to give stress and deformation results. In this study, ANSYS top-down technique is used to predict distribution of residual stress. The substrate had the following measurements: 100 mm in length, 100 mm in width, and 10 mm in height. The clad measured 2.4 mm in height and 4.1 mm in breadth. The geometry for the remaining half of the 3D meshing process was determined by considering the uniformity along the weld line (Z-direction). The 3D Solid 120 hexahedron element, which has eight nodes and one degree of freedom i.e., temperature at each node, was employed for thermal analysis. At each node, a mechanical analogue of the 120 solid components has three degrees of freedom (translations in X, Y, and Z directions). For thermo-mechanical modelling, the solid 120 element was changed to the solid 205 element throughout the modelling process, and thermal analysis and structural analysis were combined. The deposit of clad material on the substrate was imitated using the element birth and kill method. A moving consumable electrode that served as the process' heat source deposited heat on the substrate. The components of the armour were destroyed and rendered inactive in the model when a heat source was applied. The clad zone and a portion of the substrate towards the interface are where the heating source's heat/temperature distribution is most constrained. As a result, this section has more finely meshed than other areas. Coarser elements were gradually messed into the remaining substrate region. This kind of non-uniform mesh distribution is known as the transitional mapped mesh approach [23, 24], where a ratio between fine and coarse element size is followed. The transitory nature of the MIGC process prompted the model to do a transient coupled thermal and structural study. The simulated results are compared with the experimental work of Lai et al. [25], and a good agreement is found in the trend of residual stress values.

Results and Discussion

The residual stresses and temperature distribution resulting from the cladding have been analysed using the component birth and death feature. Convection loads are given to the top of the base material, while the

Table 3.1 Properties of material

	Density	Poison's ratio	Young's modulus	Thermal conductivity	Thermal expansion coefficient	Specific heat
Base metal	7800kg/m^3	0.3	200GPa	42W/m-K	11.6/ °C	365W
clad material	7800kg/m^3	0.3	190GPa	15W/m –K	18.6/ °C	465W

Source: Author

bottom is thermally insulated. The body is first heated to 180°C. Around 1800°C is the maximum temperature, while 180°C is the lowest. Elements that are clad are made visible by applying component birth and death characteristics. Other components are eliminated and kept out of sight. The temperature increases at the top and decreases as it moves towards the base metal. A temperature of about 180°C can be seen at the base of the foundation material. The temperatures are at their lowest outside of the cladding area.

The temperature is shown in Figure 3.1 from the top clad layer to the base material. The temperature from top to bottom on the graph is decreasing parabolic. Temperatures are highest at the top and lowest at the bottom.

Figure 3.2 depicts the growth of residual stress in the clad material. The midsection of the materials contained the most tension. Due to the differing materials, this can be a result of differential expansion and distortion. There is virtually any discernible difference in tension between the top and bottom. The analysis is carried out using a variety of thicknesses in order to examine the impact of clad layer thickness on residual stress produced.

Figure 3.3 illustrates the relationship between von Mises stress variation and cladding material thickness. With thickness, the von Mises stress is consistently rising. To discover the optimal clad material, more study is done using several materials. For comparison, aluminium, brass, and zerconium are considered. The characteristics of the clad material are altered, and analysis is done to determine the generation of residual stress.

Figure 3.4 displays the geometry-wide von Mises stress plot. Since the stiffness modulus of base metals is substantially higher than the young's modulus, the aluminium material is under the least stress.
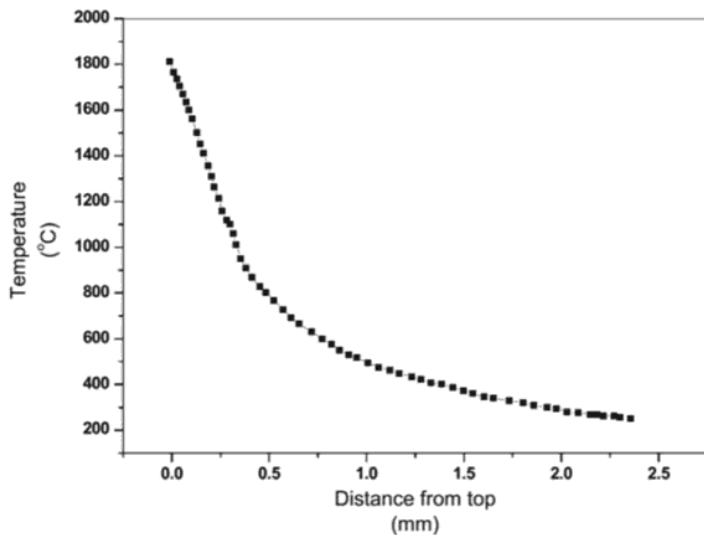

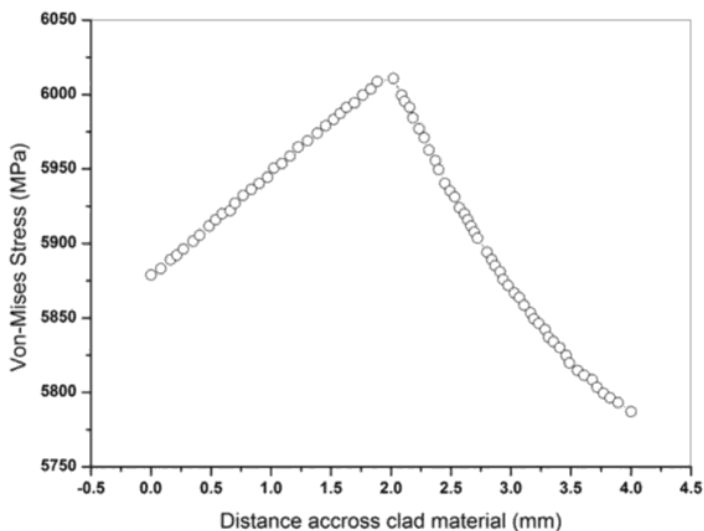*Figure 3.1* Temperature across the entire thickness
Source: Author

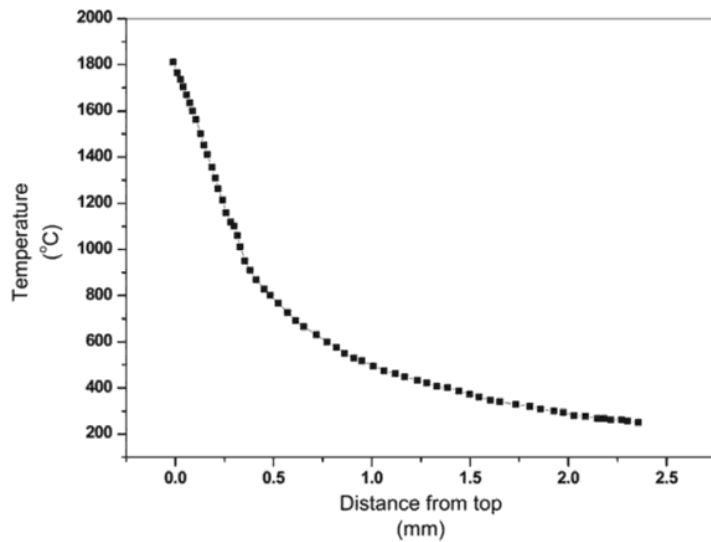*Figure 3.2* Stress distribution for the clad material
Source: Author

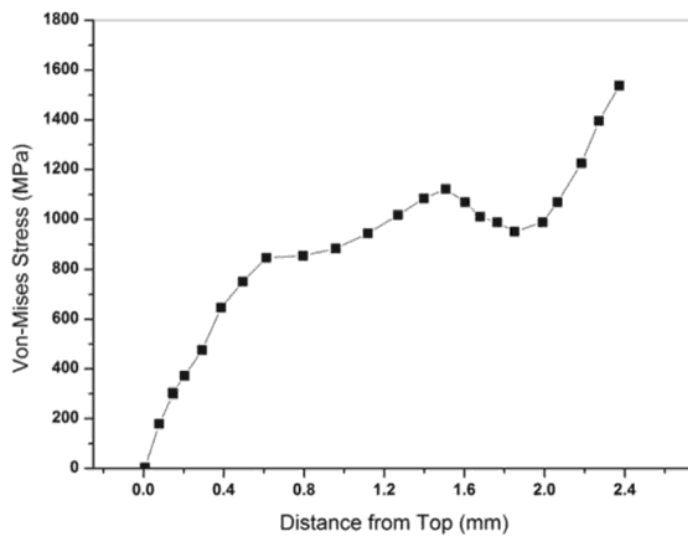*Figure 3.3* Clad thickness vs von Mises stress
Source: Author

Figure 3.4 von Mises stress graph
Source: Author

von Mises stress tension is seen in the brass cladding in Figure 3.5. Once again, the stresses in the brass material are lower than in the base material. This is mostly caused by steel having a greater Young's modulus than brass. The structure experiences additional stress production as a result of the larger thermal expansion coefficient differences. The optimum material for cladding is zirconium since it has the lowest thermal expansion coefficient among engineering materials with good mechanical qualities.

Figure 3.6 depicts residual stress in the zirconium-clad structure. The base metal has the highest stress levels, whereas zirconium exhibits the lowest. This is primarily explained by the structure's reduced stresses caused by heating, which results in a decreased thermal expansion coefficient of zirconium.

The cladding process is simulated in the current study using ANSYS and finite element analysis. To make map meshing easier, the initial clad geometry and base metal are modelled and divided. Relevant attributes are given to the mesh geometry. The whole body is first heated to 180°C. Block by block simulation of the cladding is used for further investigation. Plots of temperature are shown. The region distant from the cladding process is exposed to least temperature, while the top clad geometry is subjected to highest temperature. After 2000 sec of cooling time it returns to its starting point. By relating thermal loads to structural conditions, the study is transformed into a structural analysis. The coupled field analysis demonstrates that residual stress has built up throughout the cladding process because it shows a gradient of stress, with the lowest stress at the top and the maximum stress in the region where it is restricted. The investigation and analysis are carried out for various thicknesses in order to identify the effect of cladding material thickness on the formation of residual stress. Less clad material thickness is associated with lower residual stress.
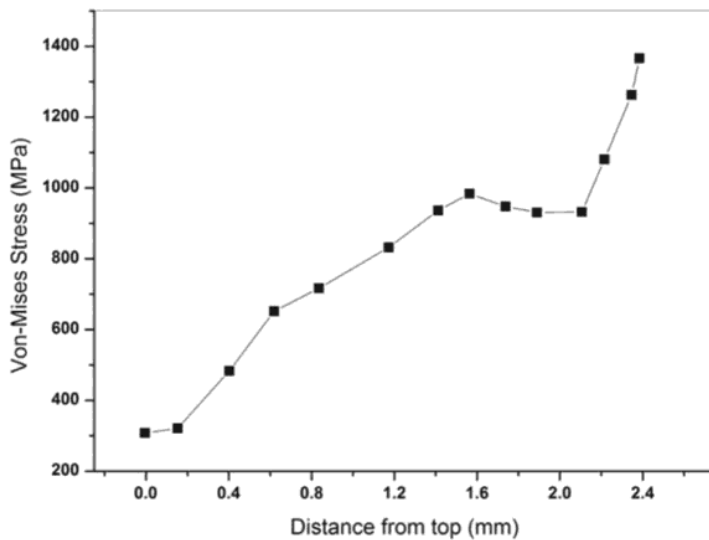
Figure 3.5 Stress diagram of brass
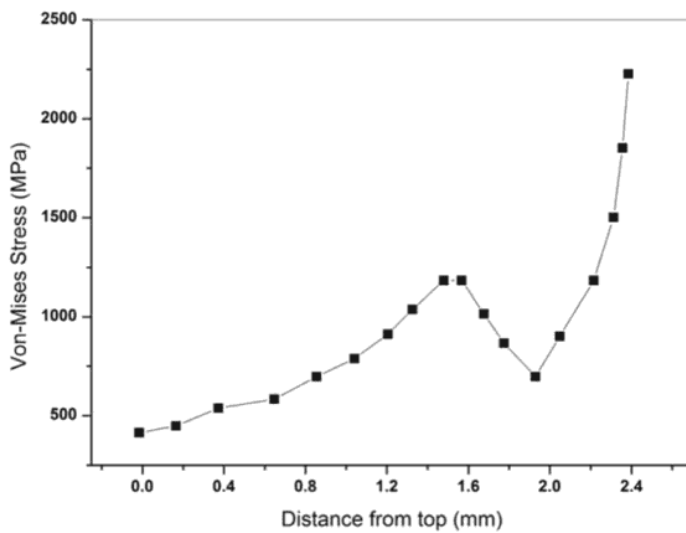*Source:* Author

Figure 3.6 Residual stress graphic plot
Source: Author

Lower heat input to the structure may be too responsible for this. Various cladding materials are used in further analysis. The findings demonstrate that materials with higher thermal expansion coefficients result in greater strains than those with lower thermal expansion coefficients. The most effectively constructed cladding material with the least amount of residual stress development in the structure is zirconium, which has a reduced thermal expansion. The amount of stress that the materials can sustain is also significantly influenced by Young's modulus.

Conclusions

The ANSYS is used to model the thermal cladding process. The distribution of temperatures throughout the cladding process, the use of component birth and death, the impact of clad material thickness, and the role of various clad materials in producing residual stress are all discussed.

- To facilitate brick meshing of the structure, the initial clad geometry and base material geometry are constructed and divided.
- Thermal boundary conditions are implemented initially with a 180° initial preheat temperature.
- The component birth and death feature together with the Newton Raphson iterative approach are used to mimic the cladding process.
- A plot is made showing the section's temperature distribution and variance.

- After being cooled to room temperature, the structure exhibits residual stress. The constraint zone exhibits the highest stresses, while the outside surface exhibits lower stresses.
- Results for residual stress formation are further analysis by altering the thickness of the clad material. The findings show that the residual stress decreases with decreasing clad material thickness. This might be explained by the cladding's thinner thickness having lower heat content.
- According to the research, zirconium is the best cladding material since it has the fewest residual stresses.
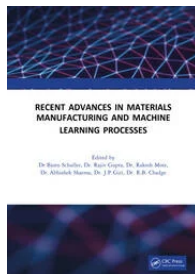
References

[1] Chang, Y. -N. and Wei, F. I. (1991). High-temperature chlorine corrosion of metals and alloys. Journal of materials science. 26(14), 3693–3698.

[2] Melchers, R. E. (2018). A review of trends for corrosion loss and pit depth in longer-term exposures. Corrosion and Materials Degradation. 1(1), 42–58.

[3] Melchers, R., E. (2019). Predicting long-term corrosion of metal alloys in physical infrastructure. Materials Degradation. 3(1), 1–7.

[4] Melchers, R., E. (2005). The effect of corrosion on the structural reliability of steel offshore structures. Corrosion Science. 47(10), 2391–2410.

[5] Cragnolino, G. (1994). Application of accelerated corrosion tests to service life prediction of materials. United States, West Conshohocken, Pennsylvania: ASTM International.

[6] Albrecht, P. and Hall, T. T. (2003). Atmospheric corrosion resistance of structural steels. Journal of Materials in Civil Engineering. 15(1), 2–24.

[7] WiseGEEK, (2016). WiseGEEK clear answers for common questions, What is Cladding? http://www.wisegeek.com/what-is cladding.htm.

[8] Lee, J. W., Nishio, K., Katoh, M., Yamaguchi, T., and Mishima, K. (2005). The performance of wear resistance cladding layer on a mild steel plate by electric resistance welding, welding in the world. 49(9/10), 94–101.

[9] Palani, P. K. and Murugan, N. (2006). Development of mathematical models for prediction of weld bead geometry in cladding by flux cored arc welding. International Journal of Advanced Manufacturing Technology. 30, 669–6.

[10] Saha, M. K. and Das, S.A. (2016). Review on different cladding techniques employed to resist corrosion. Journal of the Association of Engineers India. 86(1-2), 51–63.

[11] Chakrabarti, B., Das, S., Das, H. and Pal, T. K. (2013). Effect of process parameters on clad quality of Duplex Stainless steel using GMAW process. Transactions of the Indian Institute of Metals. 66(3), 221–230

[12] Dreilich, T., V., Assis, K. S., de Sousa, F. V. V., and de Mattos, O. R. (2014). Influence of multipass pulsed gas metal arc welding on corrosion behaviour of a duplex stainless steel. Corrosion Science. 86, 268–74. doi: https://doi.org/10.1016/j.co rsci.2014.06.004.

[13] Elango, P. and Balaguru, S. (2015). Welding parameters for inconel 625 overlay on carbon steel using GMAW. Indian Journal of Science & Technology. 8(31), 1–5.

[14] Ghosh, P. K., Gupta, P.C. and Goyal, V. K. (1998).Stainless steel cladding of structural steel plate using pulsed current GMAW process. Welding Journal. 7(7), 307–12

[15] Ibrahim, T., Yawas, D. S., and Aku, S. Y. (2013). Effects of gas metal arc welding techniques on the mechanical properties of duplex stainless steel. Journal of Minerals and Materials Characterization and Engineering. 1, 222–30.

[16] Kannan, T. and Yoganandh, J. (2010). Effect of process parameters on clad bead geometry and its shape relationships of stainless steel claddings deposited by GMAW. International Journal for Advanced Manufacturing Technology, 47, 1083–1095.

[17] Kumar, V., Singh, G., and Yusufzai, M. Z. K. (2012). Effects of process parameters of gas metal arc welding on dilution in cladding of stainless steel on mild steel. MIT International Journal of Mechanical Engineering. 2(2), 127–31

[18] Murugan, N. and Parmar, R. S. (1997). Stainless steel cladding deposited by automatic gas metal arc welding. Welding Journal. 76, 391–403

[19] Zhang, Q., Xu, P., Zha, G., Ouyang, Z., and He, D. (2021). Numerical simulations of temperature and stress field of Fe-Mn-Si-Cr-Ni shape memory alloy coating synthesized by laser cladding. *Optik*, *242*, 167079.

[20] Makhnenko, O.(2019) Influence of residual stresses in the cladding zones of rpv wwer-1000 on integrity assessment, proceedings of the second international Conference on Theoretical, Applied and Experimental Mechanics (pp.341–347).

[21] Tamanna, N., I. R. Kabir, and Naher, S. (2022). "Thermo-mechanical modelling to evaluate residual stress and material compatibility of laser cladding process depositing similar and dissimilar material on Ti6Al4V alloy." Thermal Science and Engineering Progress. 31, 101283.

[22] ANSYS analysis user's manual, Version 10. Theory reference.

[23] Kabir, I. R., D. Yin, and Naher, S. (2017). 3D thermal model of laser surface glazing for H13 tool steel. In AIP Conference Proceedings. 1896(1), 130003. AIP Publishing LLC.

[24] Kabir, I. R., Yin, D., Tamanna, N., and Naher, S. (2018). Thermomechanicalmodelling of laser surface glazing for H13 tool steel. Applied Physics. A 124(3), 1–9.

[24] Lai, Y., Yue, X., and Yue, W., (2022). A study on the residual stress of the co-based alloy plasma Cladding Layer. Materials. 15(15), 5143.

Chapter

Metal inert gas cladding simulations and residual stress analysis of mild steel

By Arka Banerjee (/search?contributorName=Arka Banerjee&contributorRole=author&redirectFromPDP=true&context=ubx), Rajeev Ranjan (/search?contributorName=Rajeev Ranjan&contributorRole=author&redirectFromPDP=true&context=ubx), Manoj Kundu (/search?contributorName=Manoj Kundu&contributorRole=author&redirectFromPDP=true&context=ubx), Subhas Chandra Moi (/search?contributorName=Subhas Chandra Moi&contributorRole=author&redirectFromPDP=true&context=ubx)

Book   Recent Advances in Material, Manufacturing, and Machine Learning (https://www.taylorfrancis.com/books/mono/10.1201/9781003450252/recent-advances-material-manufacturing-machine-learning?refId=467559f7-e341-49c9-a4dd-7e1f7cf09301&context=ubx)

Edition	1st Edition
First Published	2024
Imprint	CRC Press
Pages	6
eBook ISBN	9781003450252

⌕ Share

ABSTRACT   ⌄